HHS Public Access

Author manuscript

J Cell Physiol. Author manuscript; available in PMC 2021 December 01.

Published in final edited form as:

J Cell Physiol. 2020 December ; 235(12): 9958–9973. doi:10.1002/jcp.29811.

Cre/loxP approach-mediated downregulation of Pik3c3 inhibits the hypertrophic growth of renal proximal tubule cells

Ting Liu[1], **Jialing Yuan**[1], **Caihong Dai**[1], **Jinxian Xu**[1], **Shude Li**[2], **Benjamin D. Humphreys**[3], **Daniel T. Kleven**[4,#], **Jian-Kang Chen**[1,*]

[1]Departments of Cellular Biology & Anatomy and Medicine, Medical College of Georgia, Augusta University, Augusta, GA 30912, USA

[2]Department of Biochemistry & Molecular Biology, School of Basic Medical Sciences, Kunming Medical University, Kunming, Yunnan 650500, China

[3]Division of Nephrology, Department of Medicine, Washington University School of Medicine in St. Louis, St. Louis, MO 63110, USA

[4]Department of Pathology, Medical College of Georgia, Augusta University, Augusta, GA 30912, USA

Abstract

Nephron loss stimulates residual functioning nephrons to undergo compensatory growth. Excessive nephron growth may be a maladaptive response that sets the stage for progressive nephron damage, leading to kidney failure. To date, however, the mechanism of nephron growth remains incompletely understood. Our previous study revealed activation of class III phosphatidylinositol 3-kinase (Pik3c3) in the remaining kidney after unilateral nephrectomy (UNX)-induced nephron loss, but previous studies failed to generate a *Pik3c3* gene knockout animal model. Global *Pik3c3* deletion results in embryonic lethality. Given that renal proximal tubule cells make up the bulk of the kidney and undergo the most prominent hypertrophic growth after UNX, in this study we used Cre-loxP-based approaches for the first time demonstrated that tamoxifen-inducible *SLC34a1 promoter-driven CreER*^{T2} recombinase-mediated downregulation of Pik3c3 expression in renal proximal tubule cells alone is sufficient to inhibit UNX- or amino acid-induced hypertrophic nephron growth. Furthermore, our mechanistic studies unveiled that the *SLC34a1-CreER*^{T2} recombinase-mediated Pik3c3 downregulation inhibited UNX- or amino acid-stimulated lysosomal localization and signaling activation of mechanistic target of rapamycin complex 1 (mTORC1) in the renal proximal tubules. Moreover, our additional cell culture experiments using RNAi confirmed that knocking down Pik3c3 expression inhibited amino acid-stimulated mTORC1 signaling and blunted cellular growth in primary cultures of renal proximal tubule cells. Together, both our *in vivo* and *in vitro* experimental results indicate that Pik3c3

[*]**To whom correspondence should be addressed:** Dr. Jian-Kang Chen, Departments of Cellular Biology & Anatomy and Medicine, Medical College of Georgia at Augusta University, 1459 Laney Walker Boulevard, CB2202, Augusta, Georgia 30912, USA, Phone: 706-721-8424, Fax: 706-721-7661, JCHEN@augusta.edu.

[#]Present address: Dr. Daniel T. Kleven, Department of Pathology, Wake Forest School of Medicine, Wake Forest Baptist Medical Center, Winston-Salem, NC 27157, USA.

Data Availability Statement: The data sets used and/or analyzed during the current study are available from the corresponding author on reasonable request

is a major mechanistic mediator responsible for sensing amino acid availability and initiating hypertrophic growth of renal proximal tubule cells by activation of the mTORC1-S6K1-rpS6 signaling pathway.

Keywords

Class III Phosphatidylinositol-3 Kinase (Pik3c3); Renal proximal tubule cells (RPTC); Unilateral nephrectomy (UNX); Compensatory nephron hypertrophy (CNH); Mammalian target of rapamycin complex 1 (mTORC1); ribosomal protein S6 (rpS6) phosphorylation

INTRODUCTION

In humans, nephrogenesis is complete around 36 weeks of gestation (Hinchliffe, Sargent, Howard, Chan, & van Velzen, 1991), although mice continue to form new nephrons after birth until postnatal day 3 (Hartman, Lai, & Patterson, 2007). Notably, after completion of nephrogenesis, functioning nephrons in both humans and rodents respond to nephron loss by increases size and mass, but not in number (L. G. Fine & Norman, 1989; Nowinski, 1969; Tomashefsky & Tannenbaum, 1969). This type of nephron growth is called compensatory nephron hypertrophy (CNH). Although mild to moderate CNH may augment the functional capacity of the residual nephrons as compensation for the nephron loss, persistent and excessive CNH may sometime be a maladaptive response that fosters progressive nephron damage, ultimately leading to end-stage renal disease. Judiciously tempering CNH with pharmacological inhibitors may limit the relentless progression of nephron damage in various forms of chronic kidney disease (Brenner, 2002; Fogo & Ichikawa, 1991; Hostetter, 1995; Norman, 1995; Preisig, 2000; Yoshida, Fogo, & Ichikawa, 1989). To date, however, the molecular signaling mechanisms regulating CNH remain incompletely understood.

Mammals have evolved to express three structurally distinct classes of phosphatidylinositol-3 kinase (PI3K), termed class I, II, and III PI3K (Engelman, Luo, & Cantley, 2006). Class III PI3K (Pik3c3) is also known as mVps34 (originally standing for vacuolar protein sorting defective 34), which is the only PI3K evolutionarily conserved from yeast to humans (Engelman et al., 2006; Jean & Kiger, 2014; Schu et al., 1993). While class I PI3K is well studied for its role in producing phosphotidylinositol-3,4,5-triphosphate (PIP3) to mediate the biological effects of insulin and other growth factors as well as cytokines (Jean & Kiger, 2014), the field exploring the roles of class II PI3K is still in its infancy (Falasca et al., 2017). Unlike the class I and class II PI3Ks, Pik3c3 can only use phosphatidylinositol as a substrate to produce a single product, phosphatidylinositol-3-phosphate (PI3P), by specifically phosphorylating the D-3 position on the inositol ring of phosphatidylinositol (Jean & Kiger, 2014; Schu et al., 1993).

Interestingly, in our previous studies we observed increased Pik3c3 activities in the remaining kidney in response to unilateral nephrectomy (UNX)-induced nephron loss, which led us to propose the hypothetical model that Pik3c3 mediates CNH (J. K. Chen et al., 2015). However, previous studies failed to generate a *Pik3c3* gene knockout mouse model to definitively conclude whether Pik3c3 is indeed a mechanistic mediator underlying CNH (J. K. Chen et al., 2015). Germline deletion of Pik3c3 resulted in embryonic lethality

(J. K. Chen et al., 2015). It is noteworthy that many changes have been reported in the remaining kidney after UNX, but not all the changes act as a mechanism to mediate CNH (Brenner, 1985; Diezi, Michoud, Grandchamp, & Giebisch, 1976; Fagin & Melmed, 1987; L. Fine, 1986; L. G. Fine & Norman, 1989; Johnson & Vera Roman, 1966; Moskowitz & Liu, 1995; Nowinski, 1969; Pabico, McKenna, & Freeman, 1975; Reiter, 1968; Tabei, Levenson, & Brenner, 1983). For instance, UNX activates ornithine decarboxylase, which, however, does not mediate the hypertrophy of the remaining kidney (Humphreys, Etheredge, Lin, Ribstein, & Marton, 1988). Therefore, in the present study we generated tamoxifen-inducible, renal proximal tubule-specific *Pik3c3* gene knockout mice to determine whether targeting Pik3c3 in renal proximal tubules alone is sufficient to inhibit UNX-induced compensatory hypertrophy of the contralateral kidney.

MATERIALS AND METHODS

Reagents and antibodies

Pik3c3 antibodies (Z-R016) were purchased from Echelon Biosciences (Salt Lake City, UT). β-actin (4970S), p70 S6 kinase (catalog 2708), p-p70 S6K1 (catalog 9234), rpS6 (catalog 2217), and phospho-rpS6 (4858L) antibodies were from Cell Signaling Technology (Beverly, MA). Synaptopodin antibodies (BM5086p) were from Acris Antibodies GmbH (San Diego, CA). Vectastain ABC Kits (PK-6101) and fluorescein-labeled Lotus Tetragonolobus Lectin (LTL; FL-1321) were purchased from Vector Labs (Burlingame, CA). HRP-labeled goat anti-rabbit secondary antibodies (NEF812001EA) were from PerkinElmer (Waltham, MA). Alexa Fluor 594-conjugated goat anti-rabbit (A11012) and donkey anti-mouse (A21203) secondary antibodies were purchased from Invitrogen Life Technologies (Carlsbad, CA). Collagenase I and all other reagents were from Sigma-Aldrich (St Louis, MO).

Experimental animals

Mice were housed at the Augusta University veterinary facility under a 12-hour light/12-hour dark cycle with free access to water and standard mouse diet. Animal care and all experimental procedures were approved under the documented protocol #2012-0509 by the Institutional Animal Care and Usage Committee at Augusta University, and complied with the guidelines of National Institutes of Health.

Generation of tamoxifen-inducible renal proximal tubule-specific Pik3c3 gene knockout mice. Pik3c3 gene-floxed mice were generated as described previously (J. Chen, Chen, Fogo, Harris, & Chen, 2013). Briefly, two LoxP sites were inserted to flank exons 20-21 of the mouse gene *Pik3c3*, because these two exons encode the entire catalytic core and the key AsparDic acid-Fenylalanine-Glycine (DFG) motif (Walker, Perisic, Ried, Stephens, & Williams, 1999). A Frt-flanked phosphoglycerol kinase-neomycin (*PGK-Neo*)-positive selection cassette was cloned upstream of the first loxP site, and the targeting vector was designed to render all the distal exons out of reading frame so the ATP binding domain of this kinase was disrupted. These genetic manipulations resulted in a floxed *Pik3c3* allele with the Frt-flanked *PGK-Neo* cassette. Mice carrying this floxed allele were crossed with the *SLC34a1-CreER*^{T2}(+);R26R^{tdTomato}(+) knockin mouse (Kusaba, Lalli, Kramann,

Kobayashi, & Humphreys, 2014) to generate tamoxifen-inducible proximal tubule-specific *Pik3c3* gene knockout mice (referred to as *Pik3c3*$^{Neo\text{-ptKO}}$ mice) to compare with *SLC34a1-CreER*^{T2}-negative control (*Pik3c3*$^{Neo\text{-Ctrl}}$) mice, as illustrated in Figure 1a.

PCR primers and genotyping

Genomic DNA was isolated from mouse ear biopsy samples for PCR genotyping. 5'-CTGGACGTAAACTCCTCTTCAGACC-3' and 5'-CTAGCTTTCGGAGTCTCAGTGCAGC-3' are the sequence of PCR primers used for the floxed-*Pik3c3* allele. 5'-TTGCCTGCATTACCGGTCGATGCAACGAGT-3', 5'-CCTGGTCGAAATCAGTGCGTTCGAACGCTA-3', 5'-ACAAAACCCTACTGGGTGGA-3' and 5'-CTCGCTGTAGGACATCAT-3' were for *SLC34a1-CreER*^{T2}. 5'-AAGGGAGCTGCAGTGGAGTA-3', 5'-CCGAAAATCTGTGGGAAGTC-3', 5'-GGCATTAAAGCAGCGTATCC-3' and 5'-CTGTTCCTGTACGGCATGG-3' were for *R26R*^{tdTomato}. The PCR conditions were: 94°C for 1 min followed by 94°C for 10 s, 60°C for 30 s, and 72°C for 60 s for 30 cycles, with an additional 7-min extension at 72°C.

Induction and measurement of compensatory nephron hypertrophy

Unilateral nephrectomy (UNX) is the gold standard model for induction of CNH without causing inflammation or other confounding factors in the remaining kidney (L. Fine, 1986; Nowinski, 1969). Also, previous studies indicate that females develop considerably less hypertrophy than males after UNX (Mulroney, Woda, Johnson, & Pesce, 1999). Therefore, in the present study we used adult male mice (8 weeks of age) to induce compensatory nephron hypertrophy (CNH) by right UNX with right sham-operated mice for controls, as we described previously (J. K. Chen, Chen, Neilson, & Harris, 2005). CNH was measured by the absolute values of kidney weight and kidney-to-body weight ratio as well as the widely used percentage increases in kidney-to-body weight ratio and renal protein-to-DNA ratio relative to that of sham-operated mice 7 days after the surgery when the majority of CNH is complete (J. K. Chen et al., 2005; Xu, Chen, Dong, Meyuhas, & Chen, 2015).

Morphometric analyses of renal proximal tubular and glomerular size

Among all the nephron segments, the proximal tubule undergoes the most prominent hypertrophy in response to UNX (Arataki, 1926; Hayslett, Kashgarian, & Epstein, 1968; Oliver, 1944; Trizna, Yanagawa, Bar-Khayim, Houston, & Fine, 1981). For an additional index to measure CNH, the morphometric analyses of renal proximal tubular and glomerular size were conducted as detailed previously (Xu et al., 2015). Briefly, 7 days after right UNX or sham surgery, the mice were weighed and then sacrificed to collect kidney weight. A 2-mm-thick coronal section from the mid-portion of the kidney was cut and fixed in 4% paraformaldehyde (Xu et al., 2015). Paraffin-embedded kidney sections (5 μm) were subjected to immunofluorescence staining with LTL (a specific marker for renal proximal tubules) and synaptopodin (specific for podocytes to visualize glomeruli). Five images were randomly captured at the original magnification of 100× from the LTL-positive region for each stained kidney section using the OLYMPUS IX73 inverted 2-deck platform IX73 microscope system running on the CellSens Standard software. From each image, the largest 15 proximal tubules were visually selected and their areas measured, as shown

in Supplemental Figure S1. To prevent any visual selection bias or errors, only the top 10 largest proximal tubules (based on the sorted values of the measured 15 tubules) were entered to calculate the mean values of proximal tubular area for each mouse. For glomerular size, the areas of all glomeruli highlighted by positive synaptopodin staining in each microscopic image were measured using Olympus cellSens Entry software, as shown in Supplemental Figure S2. The mean values of glomerular area were calculated for each mouse. Differences between groups were then assessed by comparing the mean values of proximal tubular and glomerular areas for mice in each group.

Immunofluorescence, immunohistochemistry, immunoblotting analysis, and treatment of mice with increased delivery of amino acids.

Immunofluorescence, immunohistochemistry, and immunoblotting analysis were performed as we have described previously (J. K. Chen, Falck, Reddy, Capdevila, & Harris, 1998; Wu et al., 2016; Xu et al., 2015). Treatment of mice with increased delivery of amino acids was conducted as described in great detail previously (J. K. Chen et al., 2015).

Assessment of kidney function

Blood urea nitrogen (BUN) and serum creatinine levels were measured as described previously (Guo et al., 2017; Wu et al., 2016; Xu et al., 2015). Briefly, mouse blood samples were collected from the retro-orbital upon euthanasia. Aliquots of the isolated serum samples were immediately used to measure BUN according to the instructions of the Liquid Urea Nitrogen Reagent Set from Pointe Scientific Inc. (Canton, MI) (Wu et al., 2016; Xu et al., 2015). Serum creatinine was measured according to the instructions of the commercial Creatinine Kit from Stanbio Laboratory (Boerne, TX) (Guo et al., 2017).

Primary cultures of mouse renal proximal tubule cells

The *SLC34a1-CreER*^{T2}(+);R26R^{tdTomato}(+) knockin mouse line expresses the *tdTomato* red fluorescent reporter specifically in differentiated renal proximal tubules after tamoxifen induction of *SLC34a1* promoter-driven *CreER*^{T2} recombinase expression (Kusaba et al., 2014). To prepare primary cultures of mouse renal proximal tubule cells, *SLC34a1-CreER*^{T2}(+);R26R^{tdTomato}(+) knockin mice were induced with tamoxifen (80 μg/g body weight by daily intraperitoneal injections for 3 consecutive days). One week after the last tamoxifen injection, the mice were euthanized and kidneys harvested aseptically. Renal proximal tubules were isolated using the previously established method (Vinay, Gougoux, & Lemieux, 1981), with some modifications. Briefly, renal cortices were dissected visually by removing the renal capsule, vessels, and medulla under sterile conditions. The dissected renal cortices were gently minced in ice-cold Krebs-Henseleit saline (KHS) solution (pH 7.4) containing 0.05% soybean trypsin inhibitor, 0.2% bovine serum albumin, 5 mM D-glucose, 1 mM L-alanine, 10 mM HEPES, 105 mM NaCl, 5 mM KCl, 24 mM $NaHCO_3$, 2 mM NaH_2PO_4, and 1.5 mM $MgSO_4$. The minced renal cortical tissues were digested in 0.15% type I collagenase at 37°C for 45 min. The digestion suspension was strained through a 100-μm sieve, washed, and centrifuged to collect the cortical fragments. The centrifugation pellet was then suspended in 45% Percoll solution prepared with 2× KHS and subjected to separation of proximal tubules by Percoll gradient centrifugation at 12,200 × g for 30 min at 4°C. The lowest band, enriched in proximal tubule segments, was washed twice with Gibco

Dulbecco's Modified Eagle's Medium/Nutrient Mixture F12 Ham (DMEM/F12) cell culture medium to remove the Percoll solution. The final proximal tubule pellet was suspended in the DMEM/F12 cell culture medium supplemented with 1% FBS (HyClone), 2.5 nM 3,3′,5-triiodo-*L*-thyronine, 50 nM hydrocortisone, 5 ng/ml selenium, 5 μg/ml insulin, 5 μg/ml transferrin, 100 U/ml penicillin, and 100 μg/ml streptomycin. The proximal tubule suspension was seeded in cell culture dishes and incubated in a 37°C, 5% CO_2, humidified cell culture incubator. The medium was changed every 2-3 days until the cells reached confluence.

Fluorescence activated cell sorting (FACS) of tdTomato red fluorescent reporter-expressing renal proximal tubule cells

After the primary cells grew out from the proximal tubule segments and reached confluence, they were sub-cultured for one passage (referred to as P1). After the P1 cells reached approximately 90% confluence, they were trypsinized and centrifuged for 5 min at 400 x g. The cell pellets were resuspended in phosphate-buffered saline (PBS) containing 2% FBS. Red fluorescence protein cell sorting was performed on the MoFlo XDP 2-laser, 7-color cell sorter using Summit software (Beckman Coulter Life Sciences). The sorted *tdTomato* red fluorescent reporter-expressing cells are renal proximal tubule cells, predominately from the S1 and S2 segments of the proximal tubule (Kusaba et al., 2014). Early passage primary cultures of mouse renal proximal tubule cells (passages 2-5) were used for subsequent experiments.

RNA interference

The siRNA transfection procedures for mouse Pik3c3 RNA interference were performed as we described previously (J. K. Chen et al., 2015). Briefly, 80% confluent mouse renal proximal tubule cells were transfected with Silencer Negative Control siRNAs (Catalog AM4611; Ambion, Life Technologies), Dharmacon SMARTpool ON-TARGETplus Mouse Pik3c3 siRNA L-063416-00-0005 (Thermo Fisher Scientific), or individual Pik3c3-specific siRNAs using the Lipofectamine reagent method (Invitrogen, Life Technologies). The 2 sets of individual siRNAs specifically target the following coding sequences of the mouse *Pik3c3* gene: GTGGCTGAAACTTCCGGTGAA and ATGGTGACGAATCATCTCCAA. siRNAs targeting these corresponding sequences of the human class III PI3K gene *PIK3C3* also silenced human class III PI3K effectively (Byfield, Murray, & Backer, 2005). Forty-eight hours after transfection, cells were made quiescent in DMEM/F-12 medium containing 0.5% FBS and 0.01× amino acids (those found in the Gibco DMEM/F-12 were defined as 1× amino acids) for 6 hours before treatment with 1× amino acids or vehicle (saline) alone for 15 minutes. The cells were quickly washed twice with ice-cold Ca^{2+}/Mg^{2+}-free PBS and lysed on ice for 30 minutes in a lysis buffer containing 1% Nonidet P-40, 50 mm NaCl, 20 mm Tris-HCl, 137 mm NaCl, 1 mm $MgCl_2$, 1 mM $CaCl_2$, 10% glycerol, 1 mm Na_3VO_4, 50 mm NaF, 1 mm PMSF, 10 μg/ml aprotinin, and 10 μg/ml leupeptin. Cell lysates were clarified at 19,400 *g* for 5 minutes at 4°C, and protein concentrations were determined by the bicinchoninic acid assay (Pierce, Life Technologies). The cell lysates were subjected to immunoblotting for proteins indicated in the relevant figures.

FACS analysis of cell size

mTORC1 activity-mediated cell size distribution was analyzed as described previously (Fingar, Salama, Tsou, Harlow, & Blenis, 2002; Kim et al., 2002), with some modifications. Briefly, renal proximal tubule cells were seeded in 6-cm dishes at 4×10^5 cells/plate and transfected with Pik3c3 siRNA or control siRNA the next day when the cells reached ~80% confluence. 24 hours after transfection, the cells were washed, trypsinized, and replated in 10-cm dishes (1:4 split) with fresh media. After culturing for an additional 48 hours (3 days after transfection), the cells were harvested for fluorescence-activated cell sorter (FACS) analysis on the FACSCalibur 2-laser 4-color flow cytometer (BD Biosciences) using CellQuest Pro software, and the mean forward scatter height (FSC-H) was determined as a measure of relative cell size. For each sample, at least 1×10^4 events were recorded.

Statistical analyses

Data are presented as means ± SEM for at least three separate experiments (each in triplicate or duplicate). An unpaired *t* test was used for statistical analyses of differences between two groups, and ANOVA with Bonferroni's *t* correction was used for multiple group comparisons using Prism 6 (GraphPad Software, http://www.graphpad.com/scientific-software/prism/). $P<0.05$ was considered statistically significant.

RESULTS

Generation of renal proximal tubule-specific Pik3c3 knockout mice

Pik3c3 is a lipid kinase, and the exons 20-21 of mouse *Pik3c3* gene encode the entire catalytic core and the key AsparDic acid-Fenylalanine-Glycine (DFG) motif (Walker et al., 1999), we therefore targeted these two critical exons. As illustrated in Figure 1a, the *Frt*-flanked phosphoglycerol kinase-neomycin (*PGK-Neo*)-positive selection cassette was inserted into the intron 19 of the *Pik3c3* gene. A first *loxP* site was cloned downstream of the second *Frt* site and upstream of exon 20, and a second *loxP* site was cloned downstream of exon 21 in the same orientation as the first *loxP* site. This created a floxed allele of mouse *Pik3c3* gene with the *Frt*-flanked *PGK-Neo* cassette. We crossed a subset of the *Pik3c3* gene-floxed mice with the *SLC34a1-CreER*^{T2}(+);R26R^{tdTomato}(+) knockin mouse (Kusaba et al., 2014) to generate tamoxifen-inducible proximal tubule-specific *Pik3c3* gene knockout mice (referred to as *Pik3c3*$^{Neo\text{-}ptKO}$ mice) for comparison with *SLC34a1-CreER*^{T2}-negative control (*Pik3c3*$^{Neo\text{-}Ctrl}$) mice, as depicted in Figure 1a.

As indicated in Figure 1b, a single dose of tamoxifen (120 mg/kg body weight by intraperitoneal injection) already effectively induced Cre-mediated recombination of the floxed *Stop* cassette, resulting in expression of the *tdTomato* red fluorescent reporter, R26R^{tdTomato}, in *Pik3c3*$^{Neo\text{-}ptKO}$ mice, but not in the *SLC34a1-CreER*^{T2}(−);R26R^{tdTomato}(+) control mice. Consistent with previous report,(Kusaba et al., 2014) the *SLC34a1-CreER*^{T2}-mediated recombination occurred solely in renal proximal tubules, particularly in the S1 and S2 segments of renal proximal tubules (Figure 1b), confirming the specificity of this mouse model.

Tamoxifen dose-dependently induced Cre-mediated reduction of Pik3c3 expression

As shown in Figure 2a, tamoxifen induced a reduction of Pik3c3 expression in *Pik3c3*^{Neo}-ptKO mice in a dose-dependent manner. It is noteworthy that 3 or 4 doses of tamoxifen (120 mg/kg body weight per dose per day) caused mild vacuolization in some of the proximal tubular cells. Furthermore, 5 doses appeared to have reached the threshold that caused more severe tubular epithelial injury (exhibiting cytoplasmic vacuolization or sloughing off and nuclear condensation, fragmentation, or disappearance) in some tubular epithelial cells. To circumvent this problem, we only used 1 dose of tamoxifen for our subsequent hypertrophy study in this mouse model, as 1 or even 2 doses did not cause any phenotype (Figure 2b).

Tamoxifen-induced Cre-mediated reduction of Pik3c3 expression in proximal tubules inhibited UNX-induced proximal tubule hypertrophy, with no effect on UNX-induced glomerular hypertrophy

There was no alteration in the body weight, left or right kidney weight, left and right kidney-to-body weight ratio, serum creatinine level, BUN level, urinary protein excretion level, and renal histology in *Pik3c3*^{Neo}-ptKO mice compared with *Pik3c3*^{Neo}-Ctrl mice after a single dose of tamoxifen injection (Supplemental Figure S3a-h). However, as shown in Figure 2a and 3a, immunoblotting consistently demonstrated a moderate reduction of Pik3c3 expression in *Pik3c3*^{Neo}-ptKO mice compared to *Pik3c3*^{Neo}-Ctrl mice in response to a single dose of tamoxifen. Immunofluorescence staining localized the moderate Pik3c3 reduction to LTL-positive proximal tubules, without affecting Pik3c3 expression in the glomerular cells (Figure 3b).

Following UNX, 25% of compensatory nephron growth derives from early and brief cellular proliferation and 75% from subsequent enlargement of tubular and glomerular cells (Johnson & Vera Roman, 1966). Importantly, one dose of tamoxifen-induced moderate reduction of Pik3c3 expression in *Pik3c3*^{Neo}-ptKO mice significantly inhibited UNX-induced CNH compared to that of *Pik3c3*^{Neo}-Ctrl mice, as revealed by decreases in right UNX-induced increases in the absolute values of left kidney weight and left kidney-to-body weight ratio in *Pik3c3*^{Neo}-ptKO mice compared with *Pik3c3*^{Neo}-Ctrl mice in response to UNX (Table 1). As additional hypertrophy indices, UNX-induced percentage increases in kidney-to-body weight ratio (Figure 3c) and renal protein-to-DNA ratio (Figure 3d) were also significantly inhibited in *Pik3c3*^{Neo}-ptKO mice, compared with *Pik3c3*^{Neo}-Ctrl mice. Furthermore, hematoxylin and eosin staining of kidney sections revealed that compared with Sham-operated *Pik3c3*^{Neo}-Ctrl mice, uninephrectomized *Pik3c3*^{Neo}-Ctrl mice appeared to have enlarged renal tubules and glomeruli. However, only UNX-induced enlargement of renal tubules, but not that of glomeruli, was inhibited in uninephrectomized *Pik3c3*^{Neo}-ptKO mice (Figure 4a). To quantitatively determine this inhibitory effect, we performed immunofluorescence staining with LTL (a specific marker to visualize proximal tubules) and a synaptopodin antibody (specific for podocytes to highlight glomeruli), as shown in Figure 4b. The stained sections were subjected to measurement of proximal tubular and glomerular size using our recently established morphometric analysis method (Xu et al., 2015). The measurement results confirmed that UNX-induced increases in proximal tubular area (Figure 4c), but not the increases in glomerular area (Figure 4d),

in *Pik3c3*$^{Neo\text{-ptKO}}$ mice were significantly inhibited compared to *Pik3c3*$^{Neo\text{-Ctrl}}$ mice. These data indicate that the tamoxifen-induced reduction of Pik3c3 expression in renal proximal tubules (Figure 4b) inhibited UNX-induced compensatory hypertrophy in renal proximal tubules. This inhibitory effect is consistent with the mechanistic signaling data revealing that UNX-induced rpS6 phosphorylation was markedly reduced in *Pik3c3*$^{Neo\text{-ptKO}}$ mice, compared to that of *Pik3c3*$^{Neo\text{-Ctrl}}$ mice (Figure 5a). This signaling activity reduction was confirmed by immunohistochemistry (Figure 5b), and triple immunofluorescence staining confirmed the specificity of such a reduction in renal proximal tubules, but not in LTL-negative (non-proximal tubular) cells (Figure 5c).

Tamoxifen-induced Cre-mediated reduction of Pik3c3 expression in proximal tubules prevented UNX- or amino acid infusion-induced mTOR translocation to the lysosomal membranes, explaining how UNX-induced rpS6 phosphorylation was markedly reduced in *Pik3c3*$^{Neo\text{-ptKO}}$ mice

Our recent study has documented that UNX stimulates increased renal blood flow and renal delivery of amino acids into the remaining kidney (J. K. Chen et al., 2015). Previous studies have demonstrated that amino acids activate mTORC1 by inducing mTORC1 translocation to the lysosomal membrane where the mTORC1 activator, Rheb, resides, which activates mTORC1 in association with the Rag GTPase heterodimers and the p18, p14, MP1, C7orf59 and HBXIP pentameric protein complex termed Ragulator (Rogala et al., 2019; Sancak et al., 2010; Sancak et al., 2008). It is also noteworthy that the population of mTOR at the lysosomal membrane represents mTORC1; the co-localization of mTOR with lysosome-associated membrane protein (LAMP) 1 or 2 is lost upon knockdown of the mTORC1-defining component, Raptor (Menon et al., 2014; Sancak et al., 2010). Interestingly, our new data shown in Figure 6 revealed that UNX induced a marked increase in mTOR co-localization with LAMP1 in the tubular epithelial cells of the remaining kidney compared with that seen in sham-operated *Pik3c3*$^{Neo\text{-Ctrl}}$ mice (Figure 6a), indicating that mTOR was markedly accumulated on the lysosomal membranes of renal tubular epithelial cells in response to UNX. More importantly, this UNX-induced mTOR translocation was markedly prevented, especially in the S1 proximal tubule segment, which is directly connected to the urinary pole of the Bowman's capsule of the nephron, in *Pik3c3*$^{Neo\text{-ptKO}}$ mice (Figure 6b). A similar inhibition of mTOR translocation was seen in the *Pik3c3*$^{Neo\text{-ptKO}}$ mice in response to amino acid infusion compared with amino acid infused *Pik3c3*$^{Neo\text{-Ctrl}}$ mice (*data not shown*). This finding is consistent with the results shown in Figure 1b and Figure 3b, which indicate that Cre-mediated recombination and the consequent reduction of Pik3c3 protein in *Pik3c3*$^{Neo\text{-ptKO}}$ mice occur solely in the proximal tubule, especially in the S1 and S2 segments of the proximal tubule. These data indicate that Pik3c3 is required for mTOR translocation to the lysosomal membranes to initiate mTORC1 activation, which mediates compensatory nephron hypertrophy following loss of renal mass (J. K. Chen et al., 2005; J. K. Chen, Chen, Thomas, Kozma, & Harris, 2009; J. K. Chen et al., 2015; Xu et al., 2015).

Downregulation of Pik3c3 protein expression inhibits amino acid-stimulated mTORC1 activation and cell growth in the proximal tubule cells in culture and in mice

In the immortalized renal proximal tubular epithelial cell line MCT, which was established from mice that develop autoimmune interstitial nephritis (Haverty et al., 1988), our

published study have demonstrated Pik3c3-dependant mTOR translocation to the lysosome membranes (J. K. Chen et al., 2015). We reasoned if Pik3c3-dependant mTOR translocation to the lysosome membranes is indeed a mechanistic step for amino acid-stimulated mTORC1 activation, then we would be able to demonstrate an indispensable role for Pik3c3 protein expression in mediating mTOR activation and cell growth in response to amino acids. As detailed in *Methods*, we prepared primary cultures of renal proximal tubule cells from *SLC34a1-CreER*^{T2}(+);R26R^{tdTomato}(+) knockin mice that had been injected with tamoxifen for induction of *tdTomato* red fluorescent reporter expression solely in the proximal tubule cells (Kusaba et al., 2014). Thus, using fluorescence-activated cell sorter (FACS), the *tdTomato* red fluorescent protein-expressing cells were sorted and collected as renal proximal tubule cells that were predominately derived from the S1 and S2 segments of the proximal tubule (Kusaba et al., 2014). As shown in Figure 7a, this approach enabled us to isolate renal proximal tubule cells of high purity, indicated by expression of the *tdTomato* red fluorescent reporter protein, although the expression levels may vary in individual cells in culture.

In mammalian cells, mTORC1 directly phosphorylates S6K1 at T389, leading to S6K1 activation and consequent phosphorylation of the further downstream rpS6. Thus, the S6K1 and rpS6 phosphorylation levels are widely used as readouts of mTORC1 activation, which mediates cell growth and cell size in response to nutrients such as amino acids (Burnett, Barrow, Cohen, Snyder, & Sabatini, 1998; Byfield et al., 2005; Dennis, Pullen, Kozma, & Thomas, 1996; Kim et al., 2002; Nobukuni et al., 2005; Pearson et al., 1995; Sancak et al., 2008). After UNX, although the concentrations of amino acids in the blood circulation are not changed, increased renal blood flow delivers increased amino acids into the remaining kidney (J. K. Chen et al., 2015). In the kidney, amino acids freely pass the glomerular filtration barrier but are normally reabsorbed by the proximal tubule cells. As shown in Figure 7b, our immunoblotting revealed that amino acids markedly stimulated S6K1 and rpS6 phosphorylation, indicating mTORC1 activation (Kim et al., 2002; Pearson et al., 1995; Sancak et al., 2008), in the primary cultures of renal proximal tubule cells. Interestingly, siRNA-mediated downregulation of Pik3c3 protein expression inhibited the amino acid-stimulated S6K1 phosphorylation, with a consistent and marked inhibition of the downstream rpS6 phosphorylation, compared with control siRNA-transfected cells (Figure 7b). These results were confirmed using 2 additional sets of individual siRNAs (indicated in *Methods*) that were previously demonstrated to be effective and specific for knocking down Pik3c3 (data not shown) (Nobukuni et al., 2005). Under normal growth conditions (in the presence of amino acids), inhibition of mTORC1 activity by rapamycin treatment, raptor siRNA transfection, or mTOR siRNA transfection has been demonstrated to shift cell size distributions to the left, which is widely used as a readout of a cell size reduction, in cultured cells (Fingar et al., 2002; Kim et al., 2002; Sancak et al., 2008). Of interest, we observed that inhibition of mTORC1 activity by Pik3c3 siRNA transfection shifted cell size distributions to the left, indicating a decrease in cell size, relative to that of control siRNA-transfected renal proximal tubule cells (Figure 7c).

In our previous study, we have also published that amino acid infusion stimulates mTOR translocation to the lysosomal membranes of renal proximal tubular cells in wild type mice within 30 minutes (J. K. Chen et al., 2015). Interestingly, as shown in Figure 8,

our additional *in vivo* experiments in the present study indicated that tamoxifen-induced Cre-mediated reduction of Pik3c3 expression in proximal tubules markedly reduced amino acid infusion-activated mTORC1 signaling to downstream S6K1 and rpS6 phosphorylation (Figure 8a), resulting in a significant inhibition on amino acid-induced hypertrophic kidney growth in the *Pik3c3*$^{Neo\text{-ptKO}}$ mice, indicated by a significant inhibition of amino acid-induced increases in kidney/body weight ratio (Figure 8b) and protein-to-DNA ratio (Figure 8c), compared with *Pik3c3*$^{Neo\text{-Ctrl}}$ mice. Of note, similar to the marked inhibition of UNX-induced mTOR translocation to the lysosomal membranes of renal proximal tubular cells in the kidney of *Pik3c3*$^{Neo\text{-ptKO}}$ mice shown in Figure 6, amino acid infusion-stimulated mTOR translocation was markedly prevented in *Pik3c3*$^{Neo\text{-ptKO}}$ mice (*data not shown*).

Discussion

Renal proximal tubules make up the bulk of the kidney (Kishi et al., 2019; Norman, 1995), this was visualized in the present study by immunofluorescence staining with the proximal tubule-specific marker, lectin *Lotus tetragonolobus* agglutinin (LTL) conjugated with FITC (Figure 1b). Early studies reported that after UNX, all components of the functioning nephrons in the remaining kidney may undergo a certain degree of compensatory hypertrophy (Arataki, 1926; L. G. Fine, Yanagawa, Schultze, Tuck, & Trizna, 1979; Oliver, 1944; Saphir, 1927). Our study revealed that UNX induces significant increases in protein/DNA ratio (an index of hypertrophic growth) mainly in the renal cortex, while only a slight increase in protein/DNA ratio was seen in the medulla (J. K. Chen et al., 2005). Further, the proximal tubule has been consistently demonstrated to be the nephron segment that undergoes the most prominent hypertrophy (Arrizurieta, Lipham, & Gottachalk, 1969; Hayslett et al., 1968; Oliver, 1944; Trizna et al., 1981). Thus, the hypertrophy of proximal tubules accounts for most of the hypertrophic growth of the remaining kidney after UNX (Hostetter, 1995; Norman, 1995). Given that the renal cortex is largely composed of proximal convoluted tubules (the S1 and the proximal part of S2 segments), in the present study we utilized the tamoxifen inducible *SLC34a1-CreER*^{T2}(+);R26R^{tdTomato}(+) knockin mouse (Kusaba et al., 2014), which expresses Cre-recombinase solely in differentiated renal proximal tubules (mainly in the S1 and S2 proximal tubular segments that are responsible from reabsorption of amino acids in the glomerular filtrate). Crossing this tamoxifen inducible *SLC34a1-CreER*^{T2} mouse with *Pik3c3* gene-floxed mice allowed us to delete Pik3c3 selectively in the proximal tubules in adult mice. With this mouse model, we examined the effect of proximal tubule-specific Pik3c3 deletion on UNX-induced compensatory nephron hypertrophy. Our results indicated that fully inducing the *SLC34a1-CreER*^{T2} recombinase activity (by daily intraperitoneal injections of tamoxifen at 120 mg/kg body weight for 5 consecutive days) caused tubular epithelial injury in proximal tubule-specific Pik3c3 knockout (*Pik3c3*$^{Neo\text{-ptKO}}$) mice. This precluded the use of *Pik3c3*$^{Neo\text{-ptKO}}$ mice injected with 5 doses of tamoxifen for hypertrophy studies. The cellular injury phenotypes seen in *Pik3c3*$^{Neo\text{-ptKO}}$ mice are reminiscent to what have been reported in the renal glomerular podocytes after Pik3c3 deletion in the podocytes (J. Chen et al., 2013). Given that complete Pik3c3 deletion in either renal proximal tubule cells or glomerular podocytes caused cellular vacuolization and injury, our results indicate that Pik3c3 is essential for normal cellular vesicle trafficking and cell survival. To circumvent

this problem, we only used 1 dose of tamoxifen (at 120 mg/kg body weight) for our subsequent hypertrophy study in the present study, as 1 or even 2 doses did not cause cellular vacuolization and injury or any other phenotype (Figure 2b).

Interestingly, our results indicated that UNX-induced increases in kidney weight and kidney-to-body weight ratio were significantly blunted in *Pik3c3*$^{Neo\text{-ptKO}}$ mice compared with the control (*Pik3c3*$^{Neo\text{-Ctrl}}$) mice after injection with one dose of tamoxifen. However, UNX-induced increases in kidney weight and kidney-to-body weight ratio in *Pik3c3*$^{Neo\text{-ptKO}}$ mice were only partially reversed, compared with *Pik3c3*$^{Neo\text{-Ctrl}}$ mice. Such a partial effect is consistent with the fact that *Pik3c3*$^{Neo\text{-ptKO}}$ mice injected with a single dose of tamoxifen had only a moderate reduction but not complete deletion of Pik3c3 expression. Nonetheless, when renal cortical homogenates were used for Western blotting to measure protein expression levels, we were unable to rule out the influence of glomeruli. Therefore, it is important to point out that the reduction (but not complete deletion) of Pik3c3 protein expression in *Pik3c3*$^{Neo\text{-ptKO}}$ mice occurred in the proximal tubules, but not in the glomeruli, as confirmed by immunofluorescence staining that localized the moderate Pik3c3 reduction to LTL-positive proximal tubules, without affecting Pik3c3 expression in the glomerular cells. Such a reduction of Pik3c3 expression is consistent with the UNX-induced compensatory hypertrophy results, which indicate that only proximal tubular hypertrophy, but not glomerular hypertrophy, was partially inhibited.

Our earlier study using the mTOR inhibitor, rapamycin, in wild type mice initially revealed that activation of the rapamycin-sensitive mTOR signaling pathway is an important signaling mechanism mediating the initiation of UNX-induced CNH (J. K. Chen et al., 2005). Subsequent studies by us (J. K. Chen et al., 2009) and others (Lee et al., 2007; Sakaguchi et al., 2006) indicate that mTOR activation also mediates diabetes-induced renal growth. In this regard, we specifically reported that homozygous deletion of the downstream mTOR effector, S6K1, inhibits renal hypertrophy induced by either UNX or diabetes (J. K. Chen et al., 2009). Our additional studies confirmed that phosphorylated rpS6 is a major downstream effector of the mTORC1-S6K1 signaling pathway in mediating UNX-induced CNH (Xu et al., 2015). More recently, we found that the interplay between EGFR-dependent class I phosphatidylinositol 3-kinases (PI3K) activity and the lipid phosphatase activity of PTEN tightly regulates the normal kidney size under the physiological condition through activation of the mTOR complex 2 (mTORC2)-Akt signaling pathway. However, this class I PI3K/PTEN-mTORC2-Akt pathway is not involved in UNX-induced compensatory nephron hypertrophy (J. K. Chen et al., 2015).

Interestingly, UNX stimulates an immediate and sustained increase of blood flow into the remaining kidney (Brenner, 1985; Deen, Maddox, Robertson, & Brenner, 1974; Hostetter, Olson, Rennke, Venkatachalam, & Brenner, 1981; Sigmon, Gonzalez-Feldman, Cavasin, Potter, & Beierwaltes, 2004; Valdivielso, Perez-Barriocanal, Garcia-Estan, & Lopez-Novoa, 1999), with a 16% increase still being seen after 28 days (Sigmon et al., 2004). Since the amino acids in blood circulation can freely pass the glomerular filtration barrier, the concentrations of amino acids in the luminal fluid at the very beginning of the proximal tubule are identical to those in the arterial plasma. The convoluted proximal tubule (the S1 and early S2 segments) reabsorbs > 90% of the filtered load of most amino acids

by high capacity amino acid transporters while the pars recta (late S2 and S3 segments) reabsorbs the remaining amino acids via high affinity amino acid transporters such that all the amino acids are normally reabsorbed by the proximal tubule (Barfuss & Schafer, 1979; Roigaard-Petersen & Sheikh, 1984; Schwegler, Silbernagl, Tamarappoo, & Welbourne, 1992). The renal tubular load of amino acids filtered through the glomerulus is the product of its concentration in the ultrafiltrate multiplied by the glomerular filtration rate (GFR) (Schwegler et al., 1992). Thus, after UNX, even the concentrations of plasma amino acids remain unchanged, an increase in GFR would increase renal tubular load of amino acids. Indeed, our recent study demonstrated that UNX stimulated a significant increase in blood flow into the remaining kidney. The increased renal blood flow led to increased delivery of amino acids locally in the remaining kidney. We proposed that the increased amino acids act as molecular growth signals to activate the mTORC1-S6K1 signaling pathway, driving the initiation of increased protein synthesis for the development of renal hypertrophy after UNX (J. K. Chen et al., 2015).

In addition, high-protein diets are known to induce kidney hypertrophy (Harris, Seifter, & Brenner, 1984), and a high-protein diet essentially provides a high level of circulating amino acids. Amino acids have long been recognized not only as the building blocks of proteins but also as potent stimulators of increased protein synthesis in the cells (Buse & Reid, 1975; Li & Jefferson, 1978). Subsequent studies indicate that amino acids induce S6K1 activation and rpS6 phosphorylation in a rapamycin-sensitive manner (Hara et al., 1998; Wang, Campbell, Miller, & Proud, 1998). Therefore, for additional experiments in the present study, we isolated renal proximal tubules from *SLC34a1-CreER*^{T2}(+);R26R^{tdTomato}(+) knockin mice (Kusaba et al., 2014) and prepared primary cultures that were further purified by fluorescence-activated cell sorter (FACS). This allowed us to demonstrate that siRNA silencing of Pik3c3 expression inhibited amino acid-activated mTORC1 signaling to phosphorylation of S6K1 and rpS6 in primary cultures of renal proximal tubule cells. More importantly, this Pik3c3 silencing-induced inhibition of the mTORC1-S6K1-rpS6 signaling pathway shifted the cell size distribution curve to the left, indicating a reduction of cell size. These cell culture data further suggest that Pik3c3 acts upstream of mTORC1 activation in promoting the hypertrophic growth of renal proximal tubule cells.

An interesting question is: what is the mechanism by which Pik3c3 mediates mTORC1 activation for the hypertrophic growth of renal proximal tubule cells? In this regard, it is known that the subset of mTOR co-localized with LAMP 1 or 2 at the lysosomal membrane represents the mTOR subunit of mTORC1 (Menon et al., 2014; Sancak et al., 2010). It has also been documented that the mTORC1 activator Rheb resides on the lysosomal membrane to activate mTORC1 in association with the Rag GTPase heterodimers and the pentameric protein complex termed Ragulator (Rogala et al., 2019; Sancak et al., 2010; Sancak et al., 2008). Interestingly, in a recent study we have published that Pik3c3 downregulation prevented amino acids from inducing mTOR translocation to the lysosomal membrane in the mouse cortical tubule (MCT) cells with characteristics of renal proximal tubule cells (J. K. Chen et al., 2015). We have also observed increases in renal blood flow and renal delivery of amino acids into the remaining kidney in response to UNX, and we have published that infusion of exogenous amino acids stimulates mTOR translocation to the lysosomal membranes of renal proximal tubular cells in wild type mice (J. K. Chen et al., 2015).

Our new data in the present study revealed that UNX– and amino acid infusion–induced mTOR lysosomal localization and mTORC1 signaling to rpS6 phosphorylation are reduced in response to a reduction of Pik3c3 protein expression in the renal proximal tubule cells of the *Pik3c3*$^{Neo\text{-ptKO}}$ mice, compared with *Pik3c3*$^{Neo\text{-Ctrl}}$ mice. These results indicate that Pik3c3 plays an essential role in mediating UNX– or amino acid–induced mTORC1 activation through a mechanism involving the recruitment of mTOR to its activation site — the lysosomal membranes.

In our recently published study, we have addressed the lipid kinase activity of Pik3c3 in both wild type mice and cultured cells (J. K. Chen et al., 2015). Specifically, we have documented that UNX induces increased renal blood flow and renal delivery of amino acids, leading to increased lipid kinase activity of Pik3c3 in the remaining kidney of wild type mice. We also observed increased lipid kinase activity of Pik3c3 in the kidneys of wild type mice in response to amino acid infusion. Furthermore, using siRNA interference, we demonstrated that a reduced Pik3c3 protein level parallels with a reduced Pik3c3 lipid kinase activity in cultured murine renal proximal tubule (MCT) cells in response to amino acids, suggesting that the Pik3c3 protein level well represents its lipid kinase activity in response to the availability of amino acids. Thus, to this end, we would speculate that we would see markedly reduced lipid kinase activity of Pik3c3 in the kidney of *Pik3c3*$^{Neo\text{-ptKO}}$ mice, compared with *Pik3c3*$^{Neo\text{-Ctrl}}$ mice, in response to either UNX-induced renal delivery of amino acids or infusion of exogenous amino acids, although we did not conduct the tedious and costly lipid kinase activity assay of Pik3c3 in the present study. However, to our understanding, a lack of the lipid kinase activity data here as an additional readout does not affect the conclusion of current study. Because we chose the commonly used immunoblotting analysis and immunofluorescence staining methods to measure the expression level and identify the precise nephron segment localization of the Pik3c3 protein to document its critical role in mediating mTORC1-S6K1 signaling to rpS6 phosphorylation and the consequent hypertrophic growth of renal proximal tubule cells.

In summary, currently there is no specific Pik3c3 inhibitor suitable for *in vivo* animal studies and previous studies failed to generate a *Pik3c3* gene knockout animal model to definitively conclude whether Pik3c3 plays an indispensable role in UNX-induced renal hypertrophy (J. K. Chen et al., 2015). Therefore, in the present study, we used Cre-lox-based approaches and generated tamoxifen-inducible, renal proximal tubule-specific Pik3c3 knockout adult mice, which allowed us for the first time to demonstrate that Cre recombinase-mediated Pik3c3 deletion in renal proximal tubules alone is sufficient to inhibit UNX-induced renal hypertrophy. Mechanistically, our signaling data indicated that UNX-induced mTOR lysosomal localization and thereby activation of mTORC1 signaling to rpS6 phosphorylation, which mediates UNX-induced renal hypertrophy (Xu et al., 2015), is dependent on the protein expression of Pik3c3. Given our recent demonstration of the increased availability of amino acids as molecular growth signals in the remaining kidney after UNX (J. K. Chen et al., 2015), our additional cell culture experiments using RNAi confirmed that silencing of Pik3c3 protein expression inhibited amino acid-stimulated mTORC1 activity and blunted cellular growth in the primary cultures of renal proximal tubule cells. Moreover, our additional experiments demonstrated that amino acid infusion-induced mTORC1 signaling and hypertrophic renal growth are significantly inhibited by

reducing Pik3c3 protein expression in renal proximal tubules. Together, our *in vivo* and *in vitro* experimental results from the present study led us to conclude that Pik3c3 is an upstream mediator sensing amino acid availability and thereby initiating hypertrophic growth of renal proximal tubule cells by activating the mTORC1-S6K1-rpS6 signaling pathway through a mechanism of recruiting mTOR to its activation site — the lysosomal membranes.

Supplementary Material

Refer to Web version on PubMed Central for supplementary material.

Acknowledgements

This work was supported by Start-up Funds from the Medical College of Georgia at Augusta University (to J.-K. Chen), funds from National Institutes of Health R01 grants DK83575 and DK114328 (to J.-K. Chen), and funds from the American Heart Association Predoctoral Fellowship Award #18PRE33990130 (to T. Liu).

REFERENCES

Arataki M (1926). Experimental researches on the compensatory enlargement of the surviving kidney afer unilateral nephrectomy (albino rat). Am J Anat, 36, 437–450.

Arrizurieta DM, Lipham EM, & Gottachalk CW (1969). Form and function in normal and hypertrophied nephrons. In Nowinski WW and Goss RJ (Ed.), Compensatory Renal Hypertrophy (pp. 29–42). New York and London: Academic Press.

Barfuss DW, & Schafer JA (1979). Active amino acid absorption by proximal convoluted and proximal straight tubules. Am J Physiol, 236(2), F149–162. [PubMed: 420296]

Brenner BM (1985). Nephron adaptation to renal injury or ablation. Am J Physiol, 249(3 Pt 2), F324–337. [PubMed: 3898871]

Brenner BM (2002). Remission of renal disease: recounting the challenge, acquiring the goal. J Clin Invest, 110(12), 1753–1758. [PubMed: 12488422]

Burnett PE, Barrow RK, Cohen NA, Snyder SH, & Sabatini DM (1998). RAFT1 phosphorylation of the translational regulators p70 S6 kinase and 4E-BP1. Proc Natl Acad Sci U S A, 95(4), 1432–1437. [PubMed: 9465032]

Buse MG, & Reid SS (1975). Leucine. A possible regulator of protein turnover in muscle. J Clin Invest, 56(5), 1250–1261. [PubMed: 1237498]

Byfield MP, Murray JT, & Backer JM (2005). hVps34 Is a Nutrient-regulated Lipid Kinase Required for Activation of p70 S6 Kinase. J Biol Chem, 280(38), 33076–33082. [PubMed: 16049009]

Chen J, Chen MX, Fogo AB, Harris RC, & Chen JK (2013). mVps34 deletion in podocytes causes glomerulosclerosis by disrupting intracellular vesicle trafficking. J Am Soc Nephrol, 24(2), 198–207. doi:10.1681/ASN.2012010101 [PubMed: 23291473]

Chen JK, Chen J, Neilson EG, & Harris RC (2005). Role of mammalian target of rapamycin signaling in compensatory renal hypertrophy. J Am Soc Nephrol, 16(5), 1384–1391. [PubMed: 15788477]

Chen JK, Chen J, Thomas G, Kozma SC, & Harris RC (2009). S6 Kinase 1 Knockout Inhibits Uninephrectomy- or Diabetes-induced Renal Hypertrophy. Am J Physiol Renal Physiol, 297(3), F585–593. doi:00186.2009 [pii] 10.1152/ajprenal.00186.2009 [PubMed: 19474189]

Chen JK, Falck JR, Reddy KM, Capdevila J, & Harris RC (1998). Epoxyeicosatrienoic acids and their sulfonimide derivatives stimulate tyrosine phosphorylation and induce mitogenesis in renal epithelial cells. J Biol Chem, 273(44), 29254–29261. [PubMed: 9786938]

Chen JK, Nagai K, Chen J, Plieth D, Hino M, Xu J, … Harris RC (2015). Phosphatidylinositol 3-kinase signaling determines kidney size. J Clin Invest, 125(6), 2429–2444. doi:10.1172/JCI78945 [PubMed: 25985273]

Deen WM, Maddox DA, Robertson CR, & Brenner BM (1974). Dynamics of glomerular ultrafiltration in the rat. VII. Response to reduced renal mass. Am J Physiol, 227(3), 556–562. [PubMed: 4412873]

Dennis PB, Pullen N, Kozma SC, & Thomas G (1996). The principal rapamycin-sensitive p70(s6k) phosphorylation sites, T-229 and T-389, are differentially regulated by rapamycin-insensitive kinase kinases. Mol Cell Biol, 16(11), 6242–6251. doi:10.1128/mcb.16.11.6242 [PubMed: 8887654]

Diezi J, Michoud P, Grandchamp A, & Giebisch G (1976). Effects of nephrectomy on renal salt and water transport in the remaining kidney. Kidney Int, 10(6), 450–462. [PubMed: 1011539]

Engelman JA, Luo J, & Cantley LC (2006). The evolution of phosphatidylinositol 3-kinases as regulators of growth and metabolism. Nat Rev Genet, 7(8), 606–619. [PubMed: 16847462]

Fagin JA, & Melmed S (1987). Relative increase in insulin-like growth factor I messenger ribonucleic acid levels in compensatory renal hypertrophy. Endocrinology, 120(2), 718–724. [PubMed: 3803301]

Falasca M, Hamilton JR, Selvadurai M, Sundaram K, Adamska A, & Thompson PE (2017). Class II Phosphoinositide 3-Kinases as Novel Drug Targets. J Med Chem, 60(1), 47–65. doi:10.1021/acs.jmedchem.6b00963 [PubMed: 27644332]

Fine L (1986). The biology of renal hypertrophy. Kidney Int, 29(3), 619–634. [PubMed: 2422432]

Fine LG, & Norman J (1989). Cellular events in renal hypertrophy. Annu Rev Physiol, 51, 19–32. [PubMed: 2469382]

Fine LG, Yanagawa N, Schultze RG, Tuck M, & Trizna W (1979). Functional profile of the isolated uremic nephron: potassium adaptation in the rabbit cortical collecting tubule. J Clin Invest, 64(4), 1033–1043. [PubMed: 225350]

Fingar DC, Salama S, Tsou C, Harlow E, & Blenis J (2002). Mammalian cell size is controlled by mTOR and its downstream targets S6K1 and 4EBP1/eIF4E. Genes Dev, 16(12), 1472–1487. [PubMed: 12080086]

Fogo A, & Ichikawa I (1991). Evidence for a pathogenic linkage between glomerular hypertrophy and sclerosis. Am J Kidney Dis, 17(6), 666–669. [PubMed: 2042646]

Guo C, Pei L, Xiao X, Wei Q, Chen JK, Ding HF, … Dong Z (2017). DNA methylation protects against cisplatin-induced kidney injury by regulating specific genes, including interferon regulatory factor 8. Kidney Int, 92(5), 1194–1205. doi:10.1016/j.kint.2017.03.038 [PubMed: 28709638]

Hara K, Yonezawa K, Weng QP, Kozlowski MT, Belham C, & Avruch J (1998). Amino acid sufficiency and mTOR regulate p70 S6 kinase and eIF-4E BP1 through a common effector mechanism. J Biol Chem, 273(23), 14484–14494. [PubMed: 9603962]

Harris RC, Seifter JL, & Brenner BM (1984). Adaptation of Na+-H+ exchange in renal microvillus membrane vesicles. Role of dietary protein and uninephrectomy. J Clin Invest, 74(6), 1979–1987. doi:10.1172/JCI111619 [PubMed: 6511911]

Hartman HA, Lai HL, & Patterson LT (2007). Cessation of renal morphogenesis in mice. Dev Biol, 310(2), 379–387. doi:10.1016/j.ydbio.2007.08.021 [PubMed: 17826763]

Haverty TP, Kelly CJ, Hines WH, Amenta PS, Watanabe M, Harper RA, … Neilson EG (1988). Characterization of a renal tubular epithelial cell line which secretes the autologous target antigen of autoimmune experimental interstitial nephritis. J Cell Biol, 107(4), 1359–1368. [PubMed: 3170633]

Hayslett JP, Kashgarian M, & Epstein FH (1968). Functional correlates of compensatory renal hypertrophy. J Clin Invest, 47(4), 774–799. [PubMed: 5641618]

Hinchliffe SA, Sargent PH, Howard CV, Chan YF, & van Velzen D (1991). Human intrauterine renal growth expressed in absolute number of glomeruli assessed by the disector method and Cavalieri principle. Lab Invest, 64(6), 777–784. [PubMed: 2046329]

Hostetter TH (1995). Progression of renal disease and renal hypertrophy. Annu Rev Physiol, 57, 263–278. [PubMed: 7778868]

Hostetter TH, Olson JL, Rennke HG, Venkatachalam MA, & Brenner BM (1981). Hyperfiltration in remnant nephrons: a potentially adverse response to renal ablation. Am J Physiol, 241(1), F85–93. [PubMed: 7246778]

Humphreys MH, Etheredge SB, Lin SY, Ribstein J, & Marton LJ (1988). Renal ornithine decarboxylase activity, polyamines, and compensatory renal hypertrophy in the rat. Am J Physiol, 255(2 Pt 2), F270–277. [PubMed: 3136663]

Jean S, & Kiger AA (2014). Classes of phosphoinositide 3-kinases at a glance. J Cell Sci, 127(Pt 5), 923–928. doi:10.1242/jcs.093773 [PubMed: 24587488]

Johnson HA, & Vera Roman JM (1966). Compensatory renal enlargement. Hypertrophy versus hyperplasia. Am J Pathol, 49(1), 1–13. [PubMed: 5944761]

Kim DH, Sarbassov DD, Ali SM, King JE, Latek RR, Erdjument-Bromage H, … Sabatini DM (2002). mTOR interacts with raptor to form a nutrient-sensitive complex that signals to the cell growth machinery. Cell, 110(2), 163–175. [PubMed: 12150925]

Kishi S, Brooks CR, Taguchi K, Ichimura T, Mori Y, Akinfolarin A, … Bonventre JV (2019). Proximal tubule ATR regulates DNA repair to prevent maladaptive renal injury responses. J Clin Invest, 129(11), 4797–4816. doi:10.1172/JCI122313 [PubMed: 31589169]

Kusaba T, Lalli M, Kramann R, Kobayashi A, & Humphreys BD (2014). Differentiated kidney epithelial cells repair injured proximal tubule. Proc Natl Acad Sci U S A, 111(4), 1527–1532. doi:10.1073/pnas.1310653110 [PubMed: 24127583]

Lee MJ, Feliers D, Mariappan MM, Sataranatarajan K, Mahimainathan L, Musi N, … Kasinath BS (2007). A role for AMP-activated protein kinase in diabetes-induced renal hypertrophy. Am J Physiol Renal Physiol, 292(2), F617–627. [PubMed: 17018841]

Li JB, & Jefferson LS (1978). Influence of amino acid availability on protein turnover in perfused skeletal muscle. Biochim Biophys Acta, 544(2), 351–359. [PubMed: 719005]

Menon S, Dibble CC, Talbott G, Hoxhaj G, Valvezan AJ, Takahashi H, … Manning BD (2014). Spatial control of the TSC complex integrates insulin and nutrient regulation of mTORC1 at the lysosome. Cell, 156(4), 771–785. doi:10.1016/j.cell.2013.11.049 [PubMed: 24529379]

Moskowitz DW, & Liu W (1995). Gene expression after uninephrectomy in the rat: simultaneous expression of positive and negative growth control elements. J Urol, 154(4), 1560–1565. [PubMed: 7658591]

Mulroney SE, Woda C, Johnson M, & Pesce C (1999). Gender differences in renal growth and function after uninephrectomy in adult rats. Kidney Int, 56(3), 944–953. doi:10.1046/j.1523-1755.1999.00647.x [PubMed: 10469362]

Nobukuni T, Joaquin M, Roccio M, Dann SG, Kim SY, Gulati P, … Thomas G (2005). Amino acids mediate mTOR/raptor signaling through activation of class 3 phosphatidylinositol 3OH-kinase. Proc Natl Acad Sci U S A, 102(40), 14238–14243. [PubMed: 16176982]

Norman JT, and Fine LG. (1995). Renal growth and hypertrophy. In Massry SG, and Glassock RJ (Ed.), Textbook of Nephrology (pp. 146–158). Baltimore: Williams & Wilkins.

Nowinski WW (1969). Early history of renal hypertrophy. In Nowinski WW and Goss RJ (Ed.), Compesatory renal hypertrophy (pp. 1–8). New York and London: Scademic Press.

Oliver J (1944). New directions in renal morphology: A method, its results and its future. Harvey Lecture, 40, 102–155.

Pabico RC, McKenna BA, & Freeman RB (1975). Renal function before and after unilateral nephrectomy in renal donors. Kidney Int, 8(3), 166–175. [PubMed: 1177376]

Pearson RB, Dennis PB, Han JW, Williamson NA, Kozma SC, Wettenhall RE, & Thomas G (1995). The principal target of rapamycin-induced p70s6k inactivation is a novel phosphorylation site within a conserved hydrophobic domain. Embo J, 14(21), 5279–5287. [PubMed: 7489717]

Preisig PA (2000). Renal hypertrophy and hyperplasia. In Selden DW, Giebisch G (Ed.), The Kidney (3rd ed., Vol. 1, pp. 727–748). Philadelphia: Lippincott Williams & Wilkins.

Reiter RJ (1968). Early response of the hamster kidney to cold exposure and unilateral nephrectomy. Comp Biochem Physiol, 25(2), 493–500. [PubMed: 5653705]

Rogala KB, Gu X, Kedir JF, Abu-Remaileh M, Bianchi LF, Bottino AMS, … Sabatini DM (2019). Structural basis for the docking of mTORC1 on the lysosomal surface. Science, 366(6464), 468–475. doi:10.1126/science.aay0166 [PubMed: 31601708]

Roigaard-Petersen H, & Sheikh MI (1984). Renal transport of neutral amino acids. Demonstration of Na+-independent and Na+-dependent electrogenic uptake of L-proline, hydroxy-L-proline and 5-oxo-L-proline by luminal-membrane vesicles. Biochem J, 220(1), 25–33. [PubMed: 6743264]

Sakaguchi M, Isono M, Isshiki K, Sugimoto T, Koya D, & Kashiwagi A (2006). Inhibition of mTOR signaling with rapamycin attenuates renal hypertrophy in the early diabetic mice. Biochem Biophys Res Commun, 340(1), 296–301. doi:10.1016/j.bbrc.2005.12.012 [PubMed: 16364254]

Sancak Y, Bar-Peled L, Zoncu R, Markhard AL, Nada S, & Sabatini DM (2010). Ragulator-Rag complex targets mTORC1 to the lysosomal surface and is necessary for its activation by amino acids. Cell, 141(2), 290–303. doi:10.1016/j.cell.2010.02.024 [PubMed: 20381137]

Sancak Y, Peterson TR, Shaul YD, Lindquist RA, Thoreen CC, Bar-Peled L, & Sabatini DM (2008). The Rag GTPases Bind Raptor and Mediate Amino Acid Signaling to mTORC1. Science.

Saphir O (1927). The state of the glomerulus in experimental hypertrophy of the kidneys of rabbits. Am J Path, 3, 329–342. [PubMed: 19969751]

Schu PV, Takegawa K, Fry MJ, Stack JH, Waterfield MD, & Emr SD (1993). Phosphatidylinositol 3-kinase encoded by yeast VPS34 gene essential for protein sorting. Science, 260(5104), 88–91. [PubMed: 8385367]

Schwegler JS, Silbernagl S, Tamarappoo BK, & Welbourne TC (1992). Amino Acid Transport in The Kidney. In Kilberg MS & Haussinger D (Eds.), Mammalian Amino Acid Transport (pp. 233–260). New York: Penum Press.

Sigmon DH, Gonzalez-Feldman E, Cavasin MA, Potter DL, & Beierwaltes WH (2004). Role of nitric oxide in the renal hemodynamic response to unilateral nephrectomy. J Am Soc Nephrol, 15(6), 1413–1420. [PubMed: 15153552]

Tabei K, Levenson DJ, & Brenner BM (1983). Early enhancement of fluid transport in rabbit proximal straight tubules after loss of contralateral renal excretory function. J Clin Invest, 72(3), 871–881. [PubMed: 6886008]

Tomashefsky P, & Tannenbaum M (1969). Macromolecular metabolism in renal compensatory hypertrophy. I. Protein synthesis. Lab Invest, 21(4), 358–364. [PubMed: 5343505]

Trizna W, Yanagawa N, Bar-Khayim Y, Houston B, & Fine LG (1981). Functional profile of the isolated uremic nephron. Evidence of proximal tubular "memory" in experimental renal disease. J Clin Invest, 68(3), 760–767. [PubMed: 7276170]

Valdivielso JM, Perez-Barriocanal F, Garcia-Estan J, & Lopez-Novoa JM (1999). Role of nitric oxide in the early renal hemodynamic response after unilateral nephrectomy. Am J Physiol, 276(6 Pt 2), R1718–1723. [PubMed: 10362752]

Vinay P, Gougoux A, & Lemieux G (1981). Isolation of a pure suspension of rat proximal tubules. Am J Physiol, 241(4), F403–411. [PubMed: 6119031]

Walker EH, Perisic O, Ried C, Stephens L, & Williams RL (1999). Structural insights into phosphoinositide 3-kinase catalysis and signalling. Nature, 402(6759), 313–320. [PubMed: 10580505]

Wang X, Campbell LE, Miller CM, & Proud CG (1998). Amino acid availability regulates p70 S6 kinase and multiple translation factors. Biochem J, 334 (Pt 1), 261–267. [PubMed: 9693128]

Wu H, Chen J, Xu J, Dong Z, Meyuhas O, & Chen JK (2016). Blocking rpS6 Phosphorylation Exacerbates Tsc1 Deletion-Induced Kidney Growth. J Am Soc Nephrol, 27(4), 1145–1158. doi:10.1681/ASN.2014121264 [PubMed: 26296742]

Xu J, Chen J, Dong Z, Meyuhas O, & Chen JK (2015). Phosphorylation of ribosomal protein S6 mediates compensatory renal hypertrophy. Kidney Int, 87(3), 543–556. doi:10.1038/ki.2014.302 [PubMed: 25229342]

Yoshida Y, Fogo A, & Ichikawa I (1989). Glomerular hemodynamic changes vs. hypertrophy in experimental glomerular sclerosis. Kidney Int, 35(2), 654–660. [PubMed: 2709670]

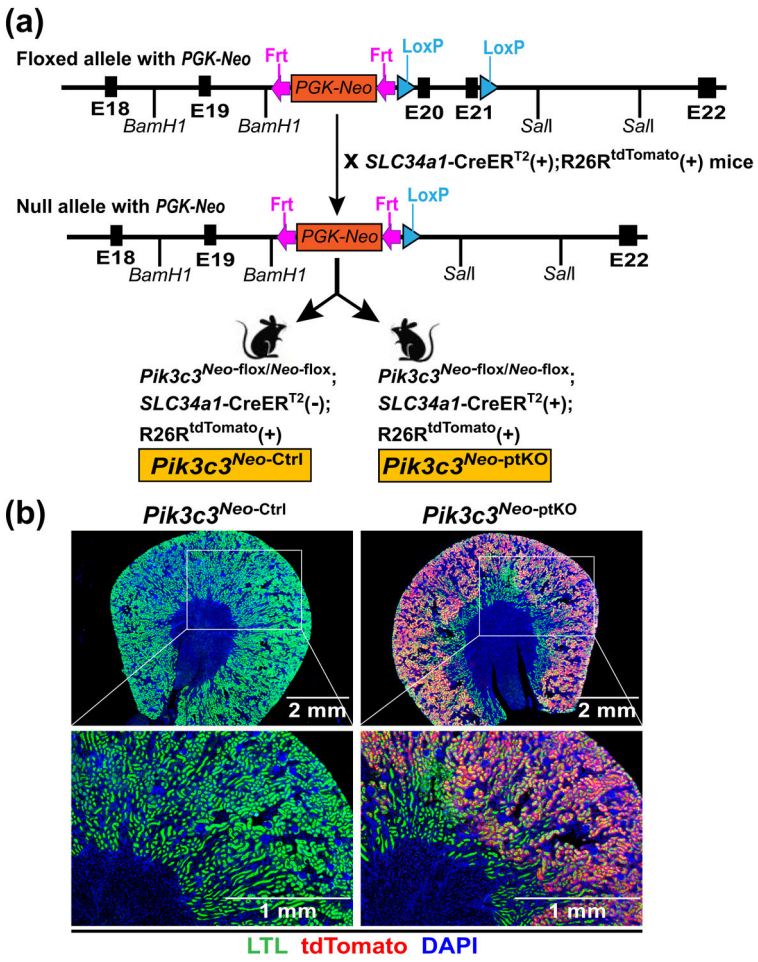

Figure 1.

Generation of tamoxifen-inducible proximal tubule-specific Pik3c3 knockout mice. (a) Strategy for generation of tamoxifen-inducible proximal tubule-specific Pik3c3 knockout mice carrying a Frt-flanked *PGK-Neo* cassette (*Pik3c3*$^{Neo\text{-ptKO}}$) to compare with their appropriate control (*Pik3c3*$^{Neo\text{-Ctrl}}$) mice, with their detailed genotypes being indicated. (b) A single dose of intraperitoneal tamoxifen injection (120 mg/kg body weight) effectively induced Cre-mediated recombination of the floxed *Stop* cassette, resulting in expression of the *tdTomato* red fluorescent reporter, R26R^{tdTomato}, in *Pik3c3*$^{Neo\text{-ptKO}}$ mice, but not in *Pik3c3*$^{Neo\text{-Ctrl}}$ mice. Note that Cre-mediated recombination occurred solely in LTL (green)-positive proximal tubules, mainly in the S1 and S2 segments of the proximal tubules residing in the renal cortex.

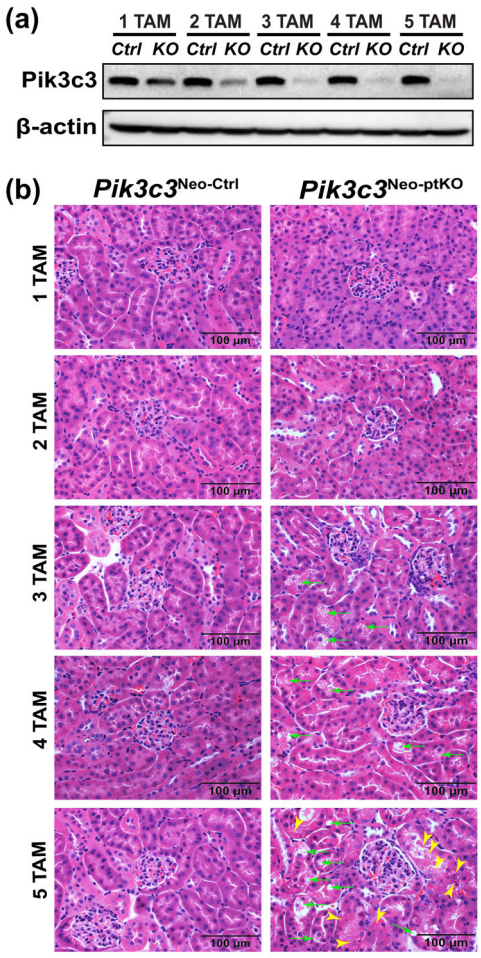

Figure 2.

Determination of the optimal tamoxifen dose for induction of *SLC34a1-CreER*^{T2}-mediated Pik3c3 deletion in renal proximal tubules. 8-week-old *Pik3c3*$^{Neo\text{-ptKO}}$ (*KO*) mice and *Pik3c3*$^{Neo\text{-Ctrl}}$ (*Ctrl*) littermates were intraperitoneally injected with different doses of tamoxifen (TAM, 120 mg/kg body weight per dose per day for 1, 2, 3, 4, or 5 consecutive days; labeled as 1, 2, 3, 4, or 5 TAM, respectively, in the figures). Two weeks after the last dose of injection, the mice were sacrificed and kidneys harvested. Renal cortical homogenates were prepared for immunoblotting with the indicated antibodies (a), revealing that tamoxifen induced Cre-mediated Pik3c3 deletion in a dose-dependent manner. Paraffin-imbedded kidney sections were also prepared and stained by H&E to examine renal histology (b). Note that 3 or 4 doses of tamoxifen injections caused mild vacuolization in some of the proximal tubular cells (green arrows), but 5 doses caused more severe tubular epithelial injury, evidenced by more severe cytoplasmic vacuolization or sloughing off (green arrows) and condensation, fragmentation or disappearance of the nuclei (yellow arrowheads) in some tubular epithelial cells of *Pik3c3*$^{Neo\text{-ptKO}}$ mice, but not in *Pik3c3*$^{Neo\text{-Ctrl}}$ littermates. However, 1 or 2 doses of tamoxifen (TAM) effectively induced a reduction of Pik3c3 expression (a) but did not cause any cellular injury (b). n = 3-5 each group with similar results.

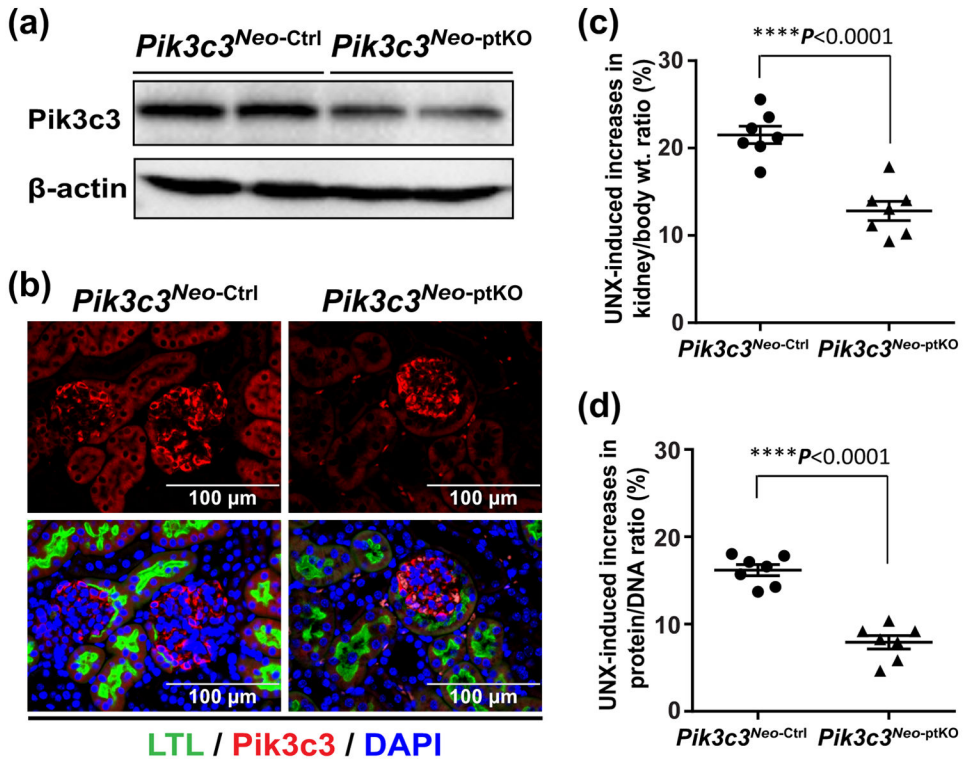

Figure 3.

Tamoxifen-induced reduction of Pik3c3 expression in renal proximal tubules attenuates UNX-induced increases in kidney/body weight ratio and protein/DNA ratio. Both 8-week-old *Pik3c3*$^{Neo\text{-ptKO}}$ mice and *Pik3c3*$^{Neo\text{-Ctrl}}$ littermates were intraperitoneally injected with one dose of tamoxifen (120 mg/kg body weight) for induction of Cre-recombinase activity 7 days before the mice were subjected to right UNX or sham surgery. 7 days after surgery, mice were sacrificed for the indicated analyses. (a) Immunoblotting analysis of renal cortical homogenates revealed a moderate reduction of Pik3c3 expression in *Pik3c3*$^{Neo\text{-ptKO}}$ mice, compared with that of *Pik3c3*$^{Neo\text{-Ctrl}}$ mice. Shown are representative blots from $n = 7$ mice per genotype group with similar results. (b) Triple immunofluorescence staining localized the moderate reduction of Pik3c3 expression to the proximal tubules, which were identified by the proximal tubule marker, LTL. (c and d) The tamoxifen-induced *SLC34a1-CreER*^{T2}-mediated reduction of Pik3c3 expression in the proximal tubules of *Pik3c3*$^{Neo\text{-ptKO}}$ mice significantly inhibited UNX-induced compensatory nephron hypertrophy, as indicated by a significant reduction in UNX-induced increases in kidney/body weight (wt.) ratio (c) and renal protein/DNA ratio (d). The values for (c and d) are means ± SEM ($n = 7$ mice per group). The *P* values in the figures were shown for the indicated comparisons.

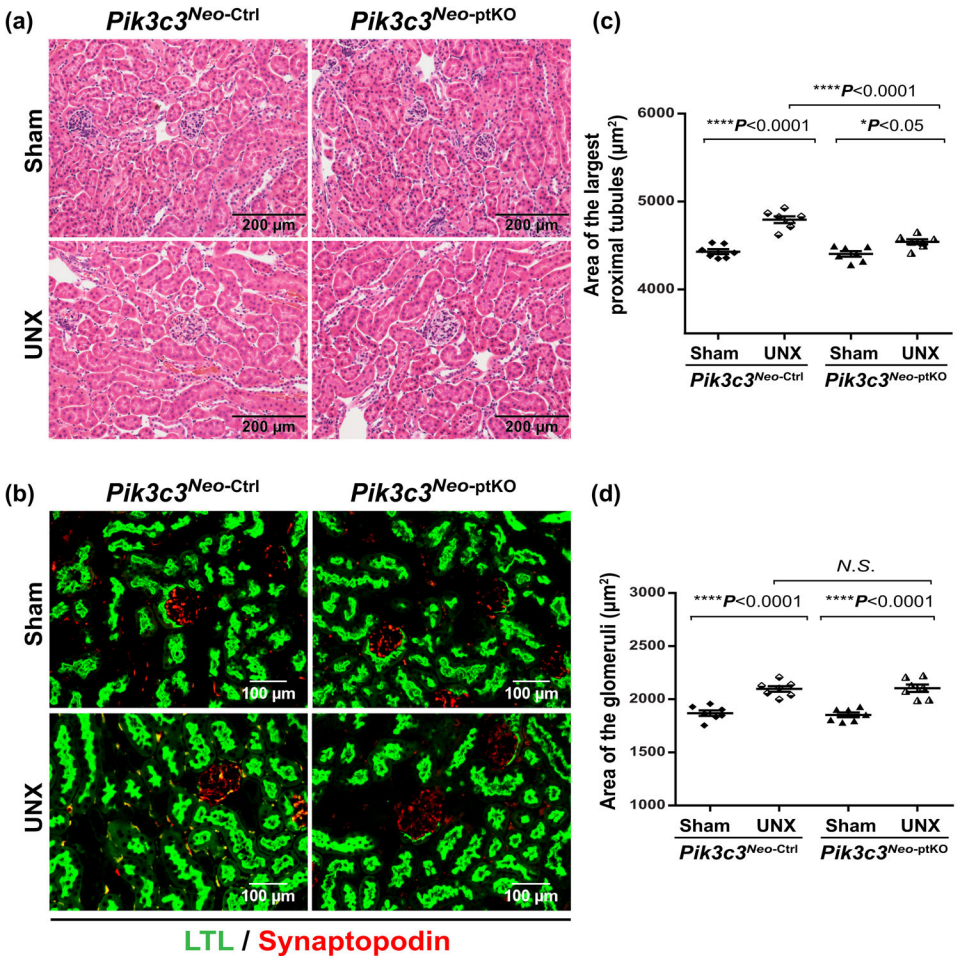

Figure 4.

Tamoxifen-induced reduction of Pik3c3 expression in renal proximal tubules inhibits the enlargement of proximal tubules, but not the enlargement of glomeruli, induced by UNX. Both *Pik3c3*$^{Neo\text{-ptKO}}$ and *Pik3c3*$^{Neo\text{-Ctrl}}$ mice were subjected to the tamoxifen induction of Cre recombinase activity and surgery as described in the legend of Figure 3. Seven days after surgery, UNX-induced proximal tubular hypertrophy and glomerular hypertrophy were assessed by kidney sections with hematoxylin and eosin stains (a) as well as double immunofluorescence stains using synaptopodin to highlight glomeruli in red and Lotus Tetragonolobus Lectin (LTL) to label renal proximal tubules in green (b). The area of proximal tubules (c) and the area of glomeruli (d) were measured as detailed in *Methods*. Values are means ± SEM ($n = 7$ mice per group), and the P values for the compared groups are indicated in the figures; *N.S.* = not statistically significant.

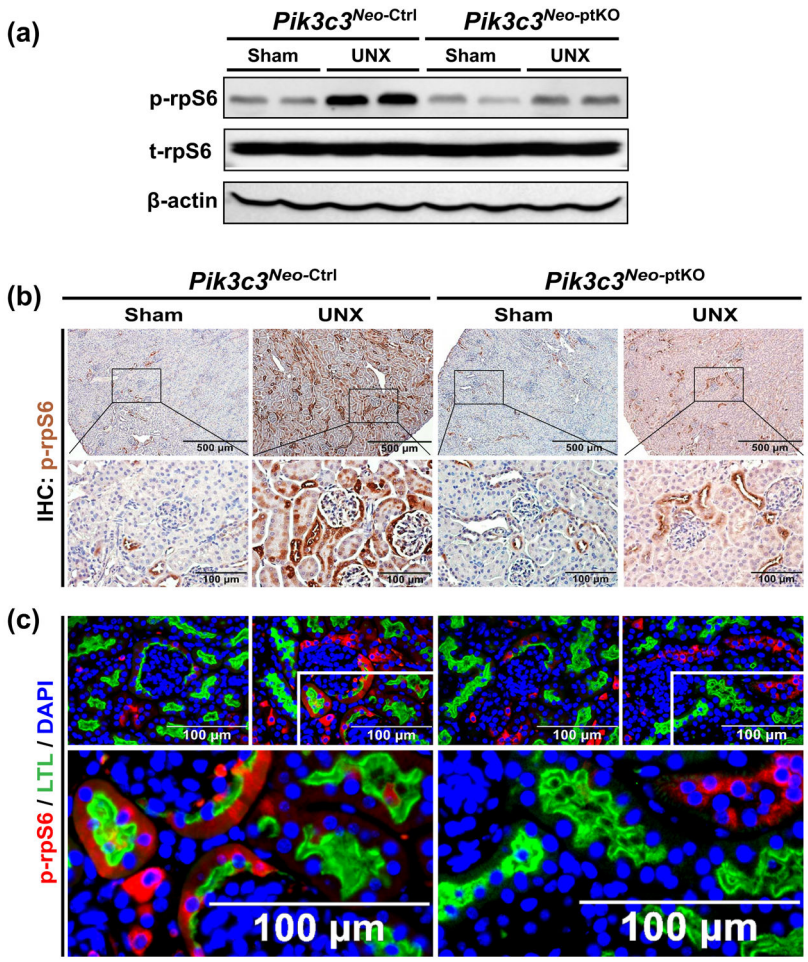

Figure 5.

Tamoxifen-induced renal proximal tubule-specific reduction of Pik3c3 expression inhibits UNX-induced rpS6 phosphorylation. Both *Pik3c3*$^{Neo\text{-ptKO}}$ and *Pik3c3*$^{Neo\text{-Ctrl}}$ mice were subjected to the tamoxifen induction of Cre recombinase activity and surgery as described in the legend of Figure 3. The mice were sacrificed and kidneys were harvested to determine the alterations of rpS6 phosphorylation by immunoblotting analysis (a) and to locate the alterations in rpS6 phosphorylation by immunohistochemistry (b) and immunofluorescence staining (c). Shown are representative blots and images from $n = 7$ mice per group with similar results.

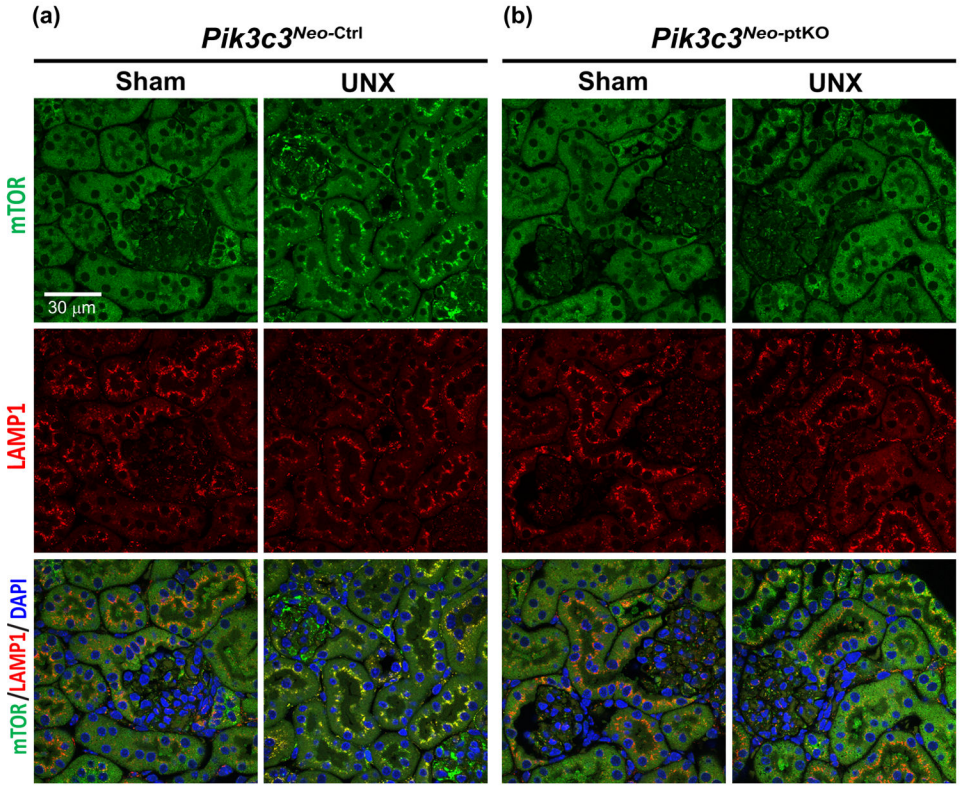

Figure 6.

Tamoxifen-induced renal proximal tubule-specific reduction of Pik3c3 expression markedly prevents UNX-induced mTOR translocation to the lysosomal membranes mainly in the S1 and S2 segments of the proximal tubules, with the S1 segment connected to the urinary pole of the Bowman's capsule of the nephrons being particularly discernible, in the remaining kidney. Both *Pik3c3*$^{Neo\text{-ptKO}}$ and *Pik3c3*$^{Neo\text{-Ctrl}}$ mice were subjected to the tamoxifen induction of Cre recombinase activity and the right surgery as described in the legend of Figure 3. Six hours after the surgery, the mice were sacrificed to harvest and process the left kidney for immunofluorescence staining and confocal microscopy to detect the localization of mTOR (green) and LAMP1 (red), with nuclei stained by DAPI (blue). Shown are representative micrographs from *n* of 5 mice per group with similar results. Scale bar: 30 μm.

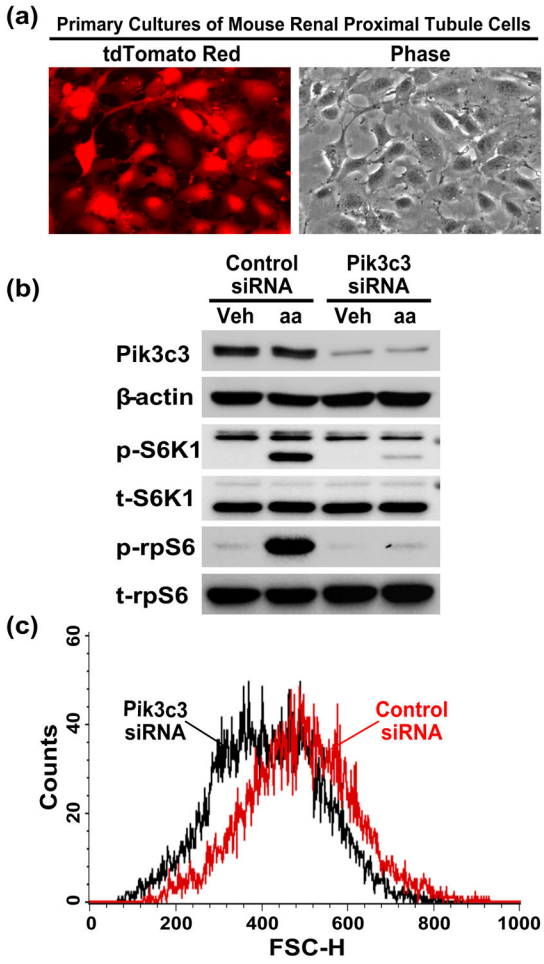

Figure 7.

Knockdown of Pik3c3 expression in primary cultures of mouse renal proximal tubules inhibits the mTOR-S6K1-rpS6 signaling pathway and shifts the cell size distribution to the left. (a) Highly pure primary cultures of renal proximal tubule cells, as indicated by the expression of red fluorescent protein, were prepared from *SLC34a1-CreER*^{T2}(+);*R26R*^{tdTomato}(+) knockin mice that express *tdTomato* red fluorescent reporter only in renal proximal tubule cells, as detailed in *Methods*. (b) The proximal tubule cells were transfected with either scrambled control siRNA or Pik3c3–specific siRNA. Forty-eight hours after transfection, the cells were made quiescent before treatment with 1× amino acids or vehicle (saline) alone for 15 minutes. Cell lysates were subjected to immunoblotting analysis to detect knockdown of Pik3c3 by siRNA and its effect on mTORC1 signaling to S6K1 and rpS6 phosphorylation. (c) The effect of Pik3c3 knockout by siRNA on cell size distribution was conducted by FACS analysis as detailed in *Methods*. The mean forward scatter height (FSC-H) was used as a measure of relative cell size, as described previously (Fingar et al., 2002; Kim et al., 2002).

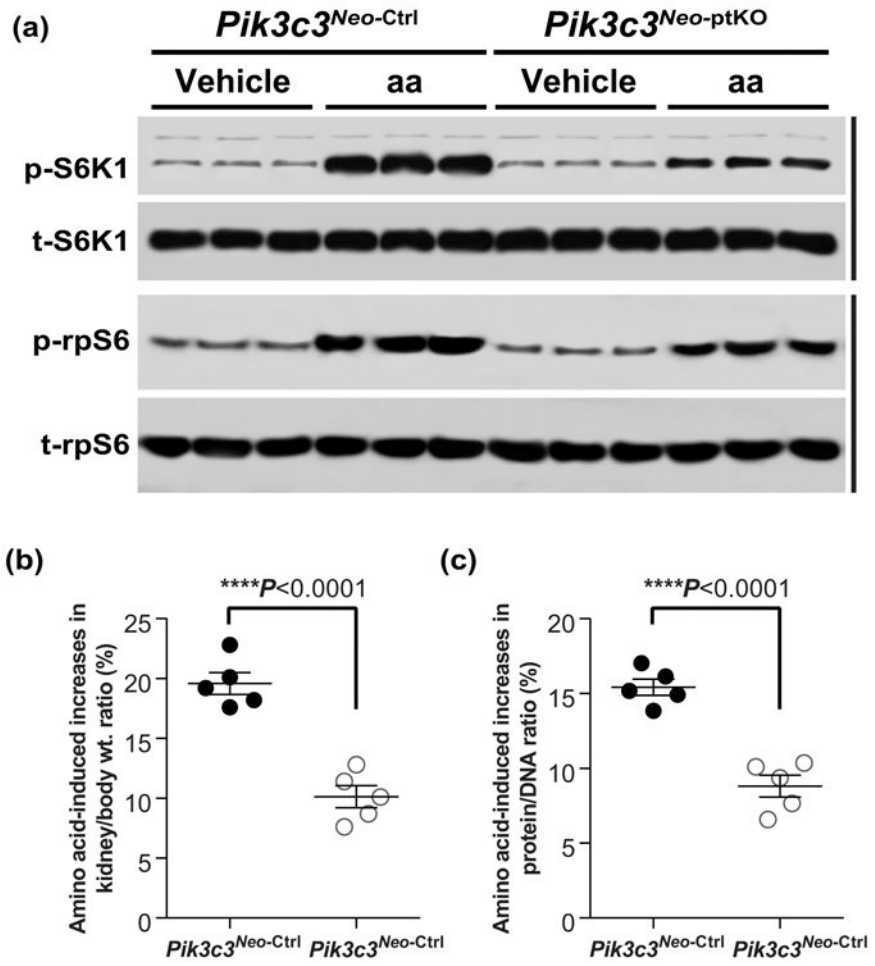

Figure 8.

Increased delivery of amino acids induces activation of the mTORC1-S6K1-rpS6 signaling pathway and hypertrophy in the kidneys of *Pik3c3*$^{Neo\text{-Ctrl}}$ mice, indicated by increases in kidney/body weight ratio and protein/DNA ratio, which are significantly inhibited in *Pik3c3*$^{Neo\text{-ptKO}}$ mice. Both *Pik3c3*$^{Neo\text{-ptKO}}$ and *Pik3c3*$^{Neo\text{-Ctrl}}$ mice were subjected to the tamoxifen induction of Cre recombinase activity as described in the legend of Figure 3. Seven days after the induction, the mice were injected through the tail vein with either 2× amino acids or vehicle (saline) control as previously described in great detail (J. K. Chen et al., 2015). 30 minutes the amino acid infusion, the mice were sacrificed and kidney samples harvested. A portion of the kidney samples were used to prepared cortical homogenates to measure mTORC1 signaling to S6K1 phosphorylation at Thr389 and rpS6 phosphorylation at Ser235/236 (a), and a slice of the harvested kidney samples were used for confocal microscopy to detect the localization of mTOR and LAMP1 as described in the legend of Figure 6 (*data not shown*). (b and c) Both *Pik3c3*$^{Neo\text{-ptKO}}$ and *Pik3c3*$^{Neo\text{-Ctrl}}$ mice were subjected to the tamoxifen induction of Cre recombinase activity as described in the legend of Figure 3. Seven days after the induction, the mice were provided with daily fresh 4× amino acids through the drinking water (13.3 ml 150× stock amino acids in 500 ml drinking water) or vehicle control (13.3 ml saline in 500 ml drinking water). After 2 weeks, the mice were sacrificed to measure amino acid-induced increases in both kidney-to-body

weight ratio (b) and renal protein-to-DNA ratio (c). A 1-tailed, unpaired t test was used for statistical analysis of the data in b and c. $n = 5$ mice per group. P values are shown in the figures to indicate specific comparisons.

TABLE 1

Body weight, left kidney weight, and left kidney/body weight ratio in *Pik3c3*$^{Neo\text{-Ctrl}}$ and *Pik3c3*$^{Neo\text{-ptKO}}$ mice 7 days after sham or uninephrectomy (UNX) surgery

Mouse genotype/ surgery	Body weight, g	Left kidney weight, g	Left kidney/body weight ratio, %
Pik3c3$^{Neo\text{-Ctrl}}$/sham	26.23±0.64	0.174±0.005	0.664±0.017
Pik3c3$^{Neo\text{-Ctrl}}$/UNX	26.03±0.46	0.210±0.004[a]	0.807±0.007[b]
Pik3c3$^{Neo\text{-ptKO}}$/sham	26.09±0.52	0.166±0.004	0.638±0.011
Pik3c3$^{Neo\text{-ptKO}}$/UNX	25.86±0.58	0.184±0.005[d]	0.711±0.006[c,e]

Values are means ± SEM (n=7 for each group). No statistical difference was seen in the body weight among the four experimental groups.

[a] $P<0.001$ *Pik3c3*^{Neo}-Ctrl/UNX vs. *Pik3c3*^{Neo}-Ctrl/sham.

[b] $P<0.0001$ *Pik3c3*^{Neo}-Ctrl/UNX vs. *Pik3c3*^{Neo}-Ctrl/sham.

[c] $P<0.001$ *Pik3c3*^{Neo}-ptKO/UNX vs. *Pik3c3*^{Neo}-ptKO/sham.

[d] $P<0.01$ *Pik3c3*^{Neo}-ptKO/UNX versus *Pik3c3*^{Neo}-Ctrl UNX.

[e] $P<0.0001$ *Pik3c3*^{Neo}-ptKO/UNX versus *Pik3c3*^{Neo}-Ctrl UNX.